MICROSTRUCTURES AND THERMO MECHANICAL PROPERTIES OF WELDED STEEL TO COPPER BY ROTARY FRICTION PROCESS

Djamel Eddine Heddar, Zakaria Boumerzoug

University of Biskra, LMSM, Department of Mechanical Engineering, BP.145, Biskra, 0700, Algeria

Corresponding author: Zakaria Boumerzoug, z.boumerzoug@univ-biskra.dz

Abstract: The objective of this work is to study the effect of rotational speed on mechanical properties and microstructural evolution of welded dissimilar metal A60 steel-copper bars by friction rotation process. Thermal behavior of the welded joint was also investigated by measuring the temperature of the central zone of the welded joint. The main techniques of characterization were tensile test and hardness measurements, optical microscopy, scanning electron microscopy equipped with energy dispersive X-ray. The obtained results indicate that an increase of rotational speed raises the temperature of the welded joint which affects its microstructural and mechanical properties.

Key words: friction welding, mechanical properties, microstructure, temperature.

1. INTRODUCTION

Joining of dissimilar metals is one of the most essential needs of industries. Friction welding is a solid state process for joining materials, especially dissimilar materials. Rotary Friction Welding (RFW) is the most commonly used method in friction welding, where welding heat is generated by friction between the surfaces of a rotating work piece and another stationary [1]. The RFW is the appropriate method for joining similar and dissimilar metals, with the advantages of no melting, short production time and low energy input [2]. The main parameters in rotary friction welding are the rotational speed, the welding time and the pressure [2,3]. Main advantages of friction welding are high material saving, low production time and possibility of welding of dissimilar metals or alloys [4].

Many research works have recently conducted investigations into the friction welding of dissimilar materials such as welding of ferrous and nonferrous alloys. For example, Sahin et al. [5] joined steel and copper using friction welding process. They determined that maximum heat is away from the center, close to but not exactly at the surface during the welding process. Shanjeevi et al.[6] investigated the effect of metallurgical properties of welded austenitic stainless steel (304L) to copper by RFW process. They found that the highest tensile strength in the friction welded joint was higher than the parent material in copper by 2.52 %. Bhagi et al. [7] studied the welded copper with carbon steel bars by RFW. They obtained that the most significant process parameters are axial pressure and rotational speed that affect the optimization of multiple performance characteristics. Fabritsiev et al. [8] found that the increase in the friction time during RFW of steel to copper by RFW causes a lower strength of the joint compared to the Cu base metal Dalip. Kumar et al. [9] jointed successfully mild steel with pure copper through friction welding under a rotation rate of 900 rpm. They found that the speed of rotation affects the intermetallic layer thickness such that a low speed of rotation results in less intermetallic layer thickness. Sahin [3], found that the formation of intermetallics at the interface is responsible for a higher hardness and lower tensile strength of the friction-welded stainless steel-copper joints.

However, the joining of steel to copper by RFW are very limited. In this present investigation, dissimilar friction welding by RFW of industrial copper and A60 steel rods was carried out. Rotational speed was varied to achieve the maximum tensile strength. Tensile tests, hardness measurements, microstructure observations, chemical composition, and thermal measurements were carried out.

2. MATERIALS AND METHODS

The materials used in the present experiment were A60 steel and industrial copper. The chemical composition and mechanical properties of these base materials are presented in Table 1 and 2.

Table 1. Chemical composition of industrial copper and A60 steel steel (Wt. %) industrial copper

Cu	Sb	Fe	Sn	Mn	Si	P	Al	Zn
97.08	2.846	0.071	0.182	0.331	0.030	0.008	0.013	0.208

C	Fe	Mo	Cu	Ni	Mn	Cr	V	Si	P
≤0.22	99.10	0.005	0.044	0.026	0.573	0.048	0.003	0.189	0.008

Table 2. Mechanical properties of steel and industrial copper

	Re (MPa)	Rm (Mpa)	Elongation A%	Hardness Vickers (HV)
A60 steel	603.3	751.0	12.2	216.0
Cu	238.1	293.2	07.0	85.5

The welding procedure was carried out on a universal milling machine PMO UF 1.5 (Made by PMO, Algeria). The friction welding conducted on the specimen dimensions of 10 mm in diameter and 80 mm in length for both base materials. Before welding, the surfaces of the bars were polished with grit paper to remove the oxide film and then cleaned with ethanol.
Friction welding process of copper bar to A60 steel bar is shown in Figure 1. The A60 steel rod was rotated and brought in contact with stationary copper rod. The welding parameters were as follows: forging force 13 kN, friction time 10 s, and rotation speed 700, 1000, and 1400 rpm.

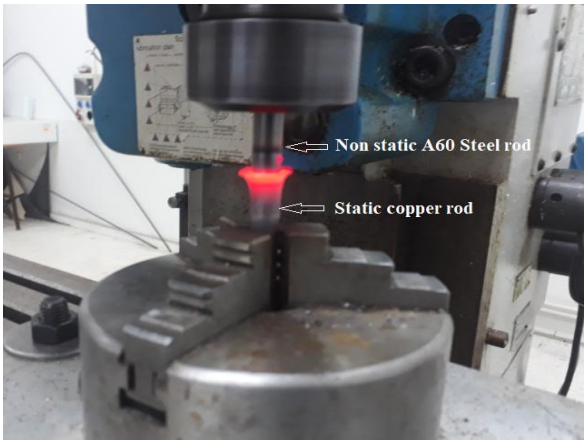

Fig.1. Friction welding of copper bar to A60 steel bar

Vickers hardness measurements were performed in the horizontal position of the boundary friction welding connection in accordance with ISO 6507-1, using hardness testing machine Matsuzawa MXT 70 instrument (Made by Matsuzawa company, Japan) with a load of 100 Kgf for copper and 300 Kgf for A60 steel. The tensile test was realized in accordance with ISO 6892-1:2016 [10], at room temperature on the universal testing machine ZWICK 1476 100KN (Made by ZWICK company, Germany). Tensile test specimens length 150 mm). Test results of tensile experiments were an average of three specimens.
For microstructural observations, samples were etched (using Nital 2 % for steel side and Nitric acid for copper side). The etched samples were observed by optical microscopy and Scanning Electron Microscopy (SEM) PHILIPS / FEI QUANTA 250, equipped with an energy dispersive X-ray (EDS) detector for chemical composition microanalysis (Made by PHILIPS/FEI company, USA). During the welding process, the temperature variations in the steel part, near the joint line, were measured by using an Infrared Video Thermometer (IRVT) device (FI 638TI) (Made by Distrame SA, France).

3. RESULTS AND DISCUSSION

3.1 Appearance of the welded joint

Figure 2 shows the appearance of copper- A60 steel joint. Joint flash was formed at the copper side which is due to the high ductility of copper. We noticed that the total length of the specimen decreased after welding process.


Fig. 2. Friction welded piece

3.2 The effect of rotational speed on temperature variation

Figure 3 shows the temperature variations in the steel part during the FRW process, measured at different rotational speeds (700, 1000, and 1400 rpm). The curves have similar shapes, increasing rapidly until reaching a maximum, then decreasing. The sated of fast increasing corresponds to the friction phase, during which the welding heat is generated by the effect of friction between the surfaces of the two bars. The axial propagation of heat along the pieces to be welded leads to a rapid increase in the temperature of the materials. The ends of this phase which correspond to the end of the rotation and consequently the end of heat generation, leading to a decrease in the temperature of the materials to be welded. The maximum peak temperature is measured for welded samples at higher rotational speed (1400 rpm) and the minimum temperature is measured at a lower rotational speed (700 rpm). The increase of the peak temperature with increasing rotational speed is due in principle to the increase in heat rate caused by increasing the friction between the two bars.

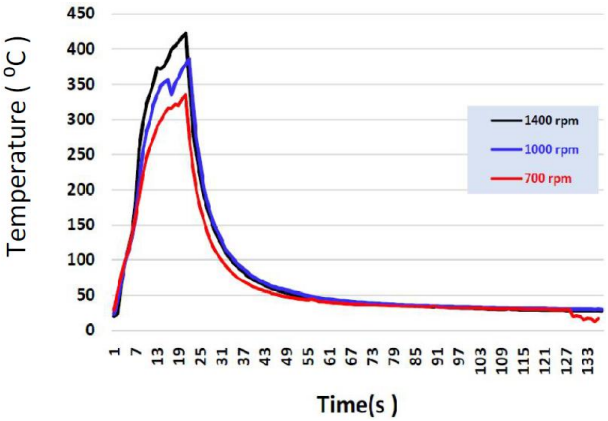

Fig. 3. Temperature variations in the A60 steel part during the welding process and under different rotational speeds (700, 1000, and 1400 rpm)

3.3 EDX analysis of the welded joints

The EDS analysis has been done on the copper side of the interface as it is shown in Figure 4. The main measured elements are Fe, Cu, and O as presented in the selected EDS spectrum among different obtained spectra (Figure 5). The EDS analysis performed on a copper side of the interface confirms the existence of the main elements, copper and iron with the presence of oxygen. The oxygen with the combination of copper or iron can form copper-oxide or iron-oxide. As mentioned by Sahin [3], the presence of intermetallic phases at the interface is obvious. In addition to that, the presence of iron in copper side confirms the diffusion of this element in copper. Lee and Jung found that diffusivity of mild steel is higher than that of copper and hence a reaction layer is formed towards copper side and the failure has taken place in this zone [11].

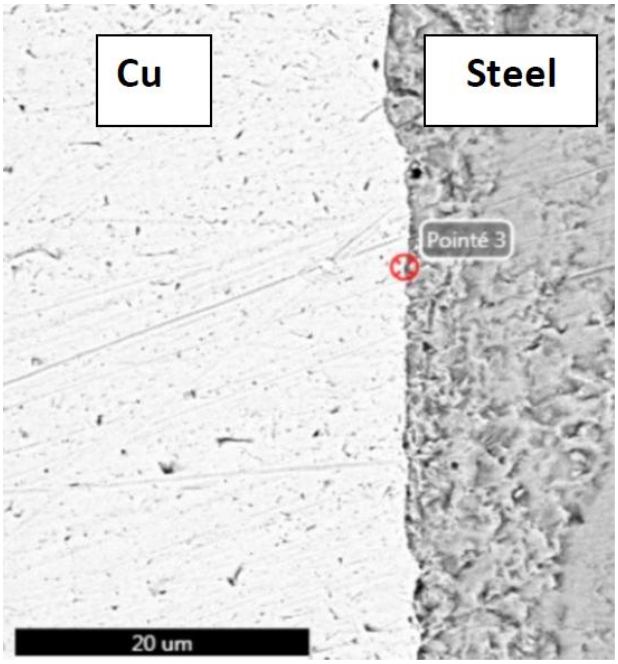

Fig. 4. Position of the EDS analysis in SEM image (indicated by cross in the interface of the welded joint Copper/ A60 steel)

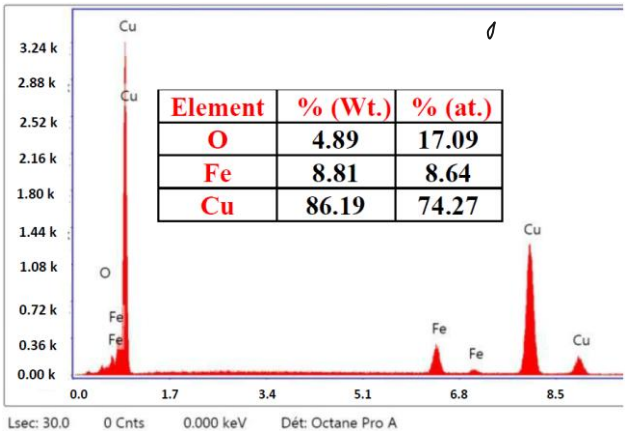

Element	% (Wt.)	% (at.)
O	4.89	17.09
Fe	8.81	8.64
Cu	86.19	74.27

Fig. 5. EDS spectrum and chemical composition of the interface in the copper side of the welded joint Copper/ A60 steel

3.4 Microstructral evolution after welding

Figure 6 shows the microstructural evolution of the welded joint after different rotational speed (700, 1000, and 1400 rpm). Along the axial direction of the welded joint by RFW, three main zones can be observed from the line contact: The central zone or the welding zone, thermal mechanical affected zone (TMAZ) and heat affected zone (HAZ). The TMAZ is the zone where heat transfers from the weld metal to the base metal. As a result, the welded joint obtained by RFW is a structurally inhomogeneous zone [12]. First of all, there is a distinction between the microstructures developed near the interface in the two parts joined. Since copper has a higher thermal conductivity than steel, the TMAZ and HAZ on the copper side are wider. In copper side, the width of TMAZ increases with the increase of the rotational speed. The dark line represents the contact line or interface between the two dissimilar materials. This interface can be the intermetallic phases as mentioned by Sahin [3]. The HAZ size is also affected by the change of the rotational speed.

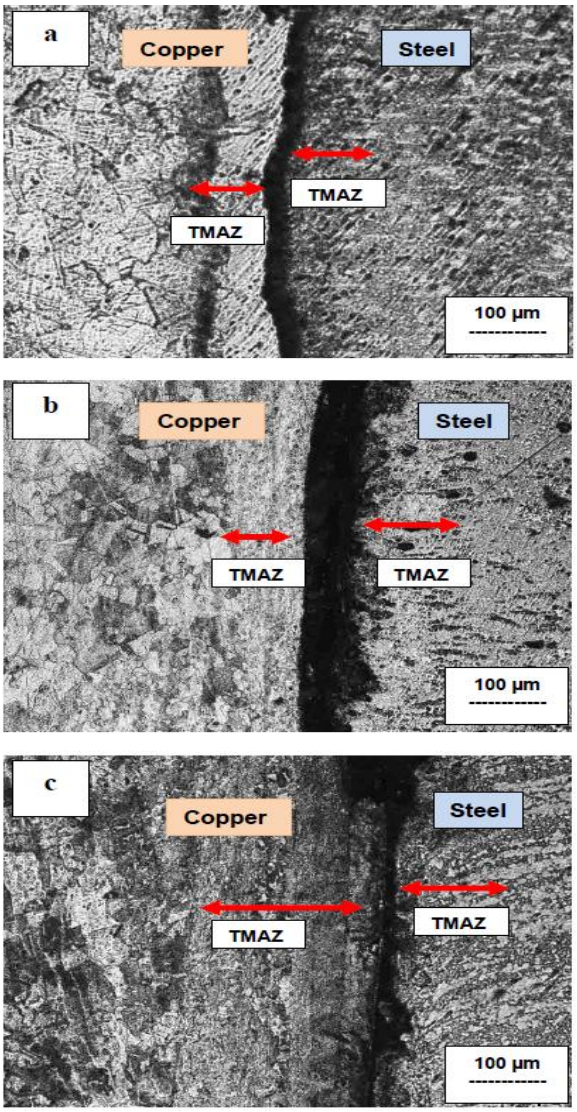

Fig. 6. Microstructural evolution of the friction welded joints copper/ A60 steel, under rotational speed of (a): 700 rpm, (b): 1000 rpm, and (c): 1400 rpm

However, some selected regions in welded jointreveals the incorporation of the two dissimilar base metals in each other as indicated by an arrow in Figure 7. This incorporation is due mainly to the ductility of copper in comparison to the steel.

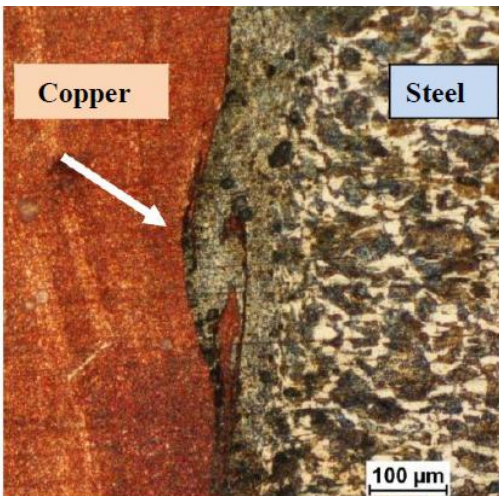

Fig. 7. Microstructural evolution of the friction welded joints copper/ A60 steel, under rotational speed of 1000 rpm

3.5 Tensile test

Figure 8 shows the macrographic view of the friction welded cooper to steel after tensile test. The rupture is located in welded joint but in the vicinity of the copper side. Joints formed here were very brittle in nature and exhibited drop in strength [11].

Fig. 8. Macrographic view of welded specimen, fractured by tensile test. Magnification of the trasversal section

The evolution of the mechanical proprieties of the welded joint after tensile tests is represented by the tensile test curves (Figure 9). The ultimate tensile stress (UTS) variation is illustrated in Figure 10. The maximum tensile strength σ_m decreases with the increase of the rotational speed. To achieve higher strength, the rotational speed should lower as possible. The highest ultimate tensile stress obtained in friction welded joint (142 MPa) was lesser than parent material of copper whose ultimate tensile stress was 293.2 MPa. This last result is in agreement with the findings of Caligulu and Acik [2]. These authors found tensile strength values of welded copper to stainless steel by RFW are lower than two base metals and all joints were fractured at the copper side. These values can be explained by rupture of welded sample in copper material as shown in Figure 10. Caligulu and Acik [2] reported that increasing bonding temperature due to the increase of the rotation speed and the friction time also promoted the growth of brittle intermetallic phase, which in turn adversely affected the bond strength. Therefore, low elongation and strength values can be attributed to presence of aligned copper precipitation reducing these properties.

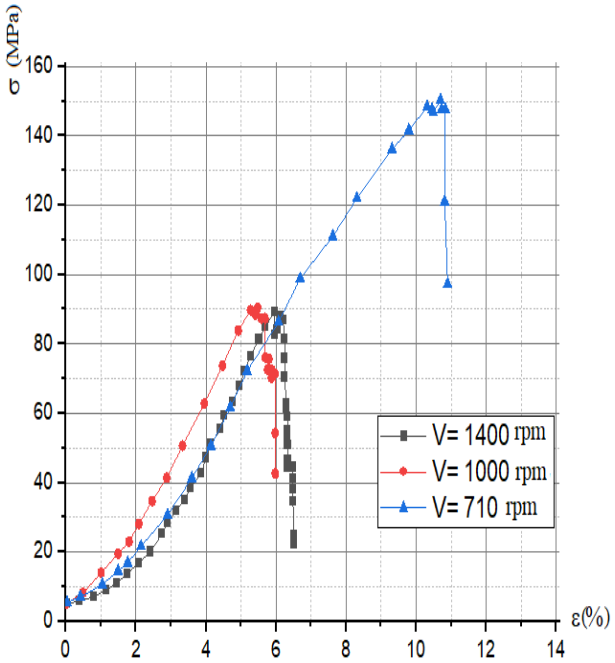

Fig. 9. Tensile test curves of the friction welded joints copper/ A60 steel, under rotational speed of (a): 700 rpm, (b): 1000 rpm and (c): 1400 rpm

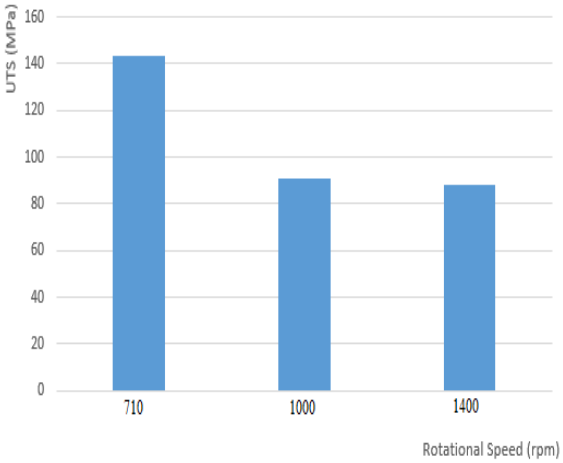

Fig. 10. Ultimate tensile stress (UTS) variation of the friction welded joints copper/ A60 steel, under rotational speed of 700 rpm, 1000 rpm, and 1400 rpm

3.6 Hardness test

It was reported that a hardness testing is the usual approach in delineating the properties of different zones in welded joint, but the information obtained is very limited [13]. For other researchers, a simple rapid way to obtain important information is by hardness testing [14]. Concerning our welded dissimilar metals, the hardness distribution across the weld region under different rotational speed is shown in Figure 11. We notice a slight decrease and decrease of the hardness in both metals after changing the rotational speed. This is due to the heat generated during the welding process and its mechanical effect on the both metals. The maximum hardness values are measured in steel side and the lower values in copper side. It is obvious that the hardness at the steel side is higher than that at the copper side. Concerning the central zone of the welded joint, which is mainly formed of the interface, thermomechanical affected zone, and heat affected zone. The hardness in this central zone varies with the variation of the rotational speed, and which can be attributed to several factors, mainly grain size, phase composition, formation of brittle intermetallics. For these raisons, the hardness values are higher due to the higher rotational speed (1000, and 1400 rpm). Comparing the hardness values with the ultimate tensile stress values, we conclude that there is not proportionality between them.

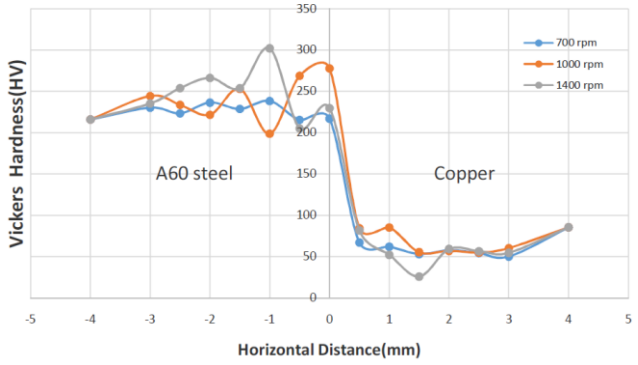

Fig. 11. Microhardness profile across the interface on friction welded joints copper/steel, under rotational speed of (a): 700 rpm, (b): 1000 rpm, and (c): 1400 rpm

4. CONCLUSIONS

In this investigation, steel and copper parts were successfully joined by RFW process. From the mechanical aspect, the maximum ultimate tensile stress of 142MPa was attained in the friction-welded joints under a rotational speed of 700 rpm. The use of high rotational speed decreases the ultimate tensile stress of joint. The maximum hardness values are measured in steel side and the lower values in copper side. The hardness values in the central zone of the welded joint are higher for the higher rotational speed, which is due to the thermomechanical effects of the friction welding. From the microstructural aspect, the microstructure observations show that in copper side, the width of thermomechanical affected zone increases with the increase of the rotational speed. The intermetallic phases at the interface are also expected to play a role in the hardness variations and tensile strength.The EDS analysis performed at a copper side of the interface confirms the existence of the main elements, copper and iron with the presence of oxygen. The oxygen with the combination of copper or iron can form copper-oxide or iron-oxide. Finally, the copper side of the welded joint is the more affected part in these dissimilar metals.

5. ACKNOWLEDGEMENTS

The authors acknowledge the Algerian Research Organism DGRSDT for their financial support of this research.

6. REFERENCES

1. Khalfallah, F., Boumerzoug, Z., Rajakumar, S., Raouache, E., (2020). *Optimization by RSM on Rotary Friction Welding of AA1100 Aluminum Alloy and Mild Steel*, Int. Review of Applied Sciences and Engineering, **11**(1), 34-42.

2. Caligulu, U., Acik, M., (2015). *Interface Characterization of Friction Welded Low Carbon Steel and Copper Alloys*, Materials Testing, **57**(1), 29-36.

3. Sahin, M., (2016). *Optimizing the Parameters for Friction Welding Stainless Steel to Copper Parts*. Materials And Technology, **50**(1), 109–115.

4. Sahin, M., (2004). *Simulation of friction welding using a developed computer program*, J.Mater. Process Technology, **153**(4), 1011–1018.

5. Sahin, AZ., Yibas, BS., Ahmed, M., Nickel, J., (1998). *Analysis of the friction welding processing relation to the welding of copper and steel bars*, J. Mater. Process Technol., **82**, 127–36.

6. Shanjeevi, C., Satish Kumar, S., Sathiya, P., (2013). *Evaluation of mechanical and metallurgical properties of dissimilar materials by friction welding*, Procedia Engineering, **64**, 1514 – 1523.

7. Bhagi, L.K., Singh, S., Singh, I., (2016). *Application of Taguchi method for optimization of continuous drive friction welding process parameters*, Ukrainian Journal of Mechanical Engineering and Materials Science, **2**(1), 1-10.

8. Fabritsiev, S.A., Pokrovsky, A.S., Nakamichi et al, M., (1998). *Irradiation resistance of DS copper/stainless steel joints fabricated by friction welding methods*, Journal of Nuclear Materials,

258(2), 2030–2035.
9. Kumar, D., Verma, A., Kulshrestha, S., Singh, P., (2013). *Microstructure and Mechanical Properties of Mild Steel Copper Joined by Friction Welding*, International Journal of Mechanical Engineering and Technology (IJMET), **4**(5), September - October, 295-300.
10. ISO 6892-1:(2019) en, *Metallic materials — Tensile testing* — Part 1: Method of test at room temperature (available in: https://www.iso.org)
11. Lee, W.B., Jung, S.B., (2003). *Effect of micro structural variation on the Cu/CK45carbon steel friction weld joints*, Z. Metallkd, **94**, pp.1300–1306.
12. Delijaicova, S., Silvaa, P.A. de O., Resendeb, H.B., Batalhab, M.H F., (2018). *Effect of Weld Parameters on Residual Stress, Hardness and Microstructure of Dissimilar AA2024-T3 and 3AA7475-T761 Friction Stir Welded Joints*, Materials Research, **21**(6), pp.1-11.
13. Stewart, G.R., Elwazri, A.M., Varano, R., Pokutylowicz, N., Yue, S., Jonas, J.J., (2006). *Shear Punch Testing of Welded Pipeline Steel*, Materials Science and Engineering, A420, pp.115-121.
14. Lars-Eric, S., (1994). *Control of Microstructures and Properties in Steel Arc Welds*, Library of Congress Cataloging - in Published Data.

Received: June 15, 2020 / Accepted: December 15, 2020 / Paper available online: December 20, 2020 © International Journal of Modern Manufacturing Technologies